

Seasonal climate summary southern hemisphere (winter 2002): consolidation of El Niño conditions in the Pacific

D.A. Jones

National Climate Centre, Bureau of Meteorology, Australia

(Manuscript received July 2003)

Southern hemisphere circulation patterns and associated anomalies for the austral winter 2002 are reviewed, with emphasis given to the Pacific Basin climate indicators and Australian rainfall and temperature patterns. Following a particularly strong westerly wind burst during May, winter 2002 witnessed the return of El Niño conditions to the Pacific Basin. By season's end, surface and subsurface ocean temperatures were significantly warmer than normal across most of the tropical Pacific Ocean, while atmospheric indicators such as cloudiness and surface pressure confirmed this shift to El Niño conditions.

Across Australia, winter 2002 was a season of exceptionally high maximum temperatures, near record low rainfall, and a record diurnal temperature range. The season as a whole witnessed the consolidation and intensification of drought conditions across most of continental Australia, marking the early stages of what was to become one of the most severe El Niño drought episodes in Australia's history.

Introduction

Following a strong westerly wind burst in May 2002, winter witnessed the rapid establishment of El Niño conditions across the Pacific Basin. By season's end, surface and subsurface temperatures were significantly warmer than average across most of the tropical Pacific Ocean, while atmospheric indicators such as cloudiness and surface pressure confirmed this shift to El Niño conditions.

This summary reviews the southern hemisphere and equatorial climate patterns for winter 2002, with particular attention given to the Australasian and Pacific Regions. The main sources of information for

this report are the Climate Monitoring Bulletin (Commonwealth Bureau of Meteorology, Australia) and the Climate Diagnostics Bulletin (Climate Prediction Center, Washington). Further details regarding sources of data are given in the Appendix.

Pacific Basin climate indices

The Troup Southern Oscillation Index*

The negative Southern Oscillation Index (SOI) values which became established in autumn 2002 (Fawcett

Corresponding author address: Dr D.A. Jones, National Climate Centre, Commonwealth Bureau of Meteorology, GPO Box 1289K, Melbourne, Vic. 3001, Australia.
Email: d.jones@bom.gov.au

*The Troup Southern Oscillation Index (SOI) used in this article is ten times the standardised monthly anomaly of the difference in mean sea-level pressure between Tahiti and Darwin. The calculation is based on a sixty-year climatology (1933-1992).

and Trewin 2003) continued through the winter season (Fig. 1) with a three-monthly mean of -9.5 , marking the first period of strongly negative values since the demise of the last El Niño in early/mid 1998. In each month the SOI was negative being -6.3 in June, -7.6 in July and -14.6 in August, with Darwin experiencing persistently above normal pressures. Tahiti experienced near normal pressures in June and July, but well below normal pressures in August. The pressure variations at both stations reflected strong intraseasonal activity, as described below.

The June/July and July/August values of the Climate Diagnostics Center Multivariate El Niño-Southern Oscillation (ENSO) Index (MEI) were $+0.55$ and $+0.84$ respectively. Such values confirm that while El Niño conditions were clearly established across the Pacific Basin by the end of winter with a coupling between the atmospheric and oceanic anomalies, the amplitude of the El Niño as represented by canonical spatial patterns was modest, and certainly much less than the 1997/98 El Niño event.

Outgoing long wave radiation

Figure 2, adapted from the Climate Prediction Center (CPC), Washington (CPC 2002), shows the standardised monthly anomaly of outgoing long wave radiation (OLR) from January 1998 to August 2002, together with a three-month moving average. These data, compiled by the CPC, are a measure of the amount of long-wave radiation emitted from an equatorial region centred about the date-line (5°S to 5°N and 160°E to 160°W). Tropical deep convection in this region is particularly sensitive to changes in the phase of the Southern Oscillation. During warm (El Niño) ENSO events, convection is generally more prevalent resulting in a reduction in OLR. This reduction is due to the lower effective black-body temperature and is associated with increased high cloud and deep convection. The reverse applies in cold (La Niña) events, with less convection expected in the vicinity of the date-line.

Across the season, tropical Pacific convection was suppressed around and north of Australia and enhanced near the date-line, consistent with the El Niño conditions which consolidated during winter. However, the mean picture is a relatively poor reflection of the within-season conditions which displayed considerable variability, as highlighted by the monthly OLR index values (-0.7 in June, $+0.5$ in July and -1.5 in August). The winter season was one of a systematic transition in anomalous tropical convection in the Pacific, with particularly strong intraseasonal activity overall.

To highlight the complexity of the OLR anomalies, Fig. 3 shows a time-longitude Hovmoller dia-

Fig. 1 Southern Oscillation Index, from January 1998 to August 2002. Means and standard deviations used in the computation of the SOI are based on the period 1933-1992.

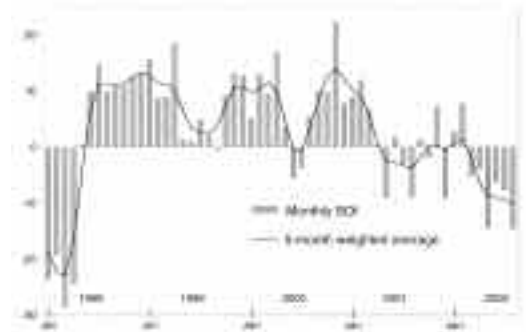
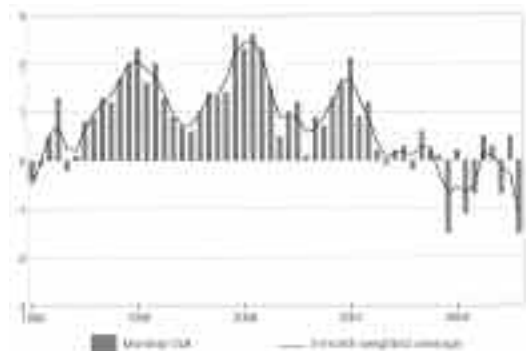
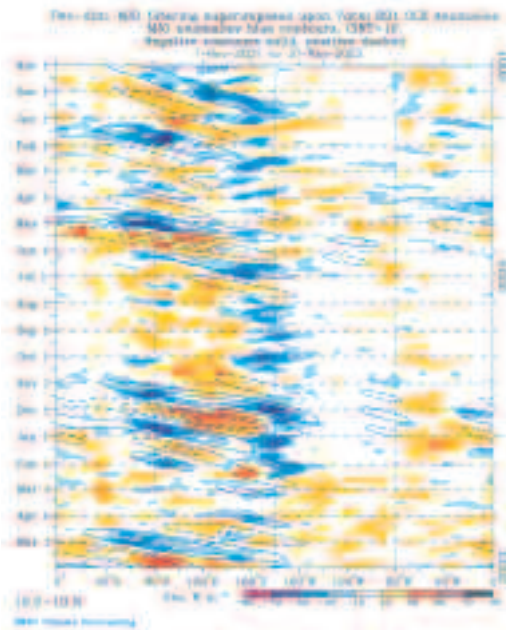


Fig. 2 Standardised anomaly of monthly outgoing long-wave radiation averaged over the area 5°S to 5°N and 160°E to 160°W , from January 1998 to August 2002. Negative (positive) anomalies indicate enhanced (reduced) convection and rainfall in the area. Anomalies are based on the 1979-1995 base period.



gram of the 7-day running mean convective anomaly for 7.5°N to 7.5°S centred on winter 2002, with the component of the convection associated with the Madden-Julian Oscillation overlaid (following Wheeler and Kiladis 1999). The convective signature of the strong westerly wind bursts in December 2001 and May 2002, followed by a weaker event during June/July 2002 (Jones 2002; Gamble 2003) is clearly evident as eastward propagating areas of enhanced (and suppressed) convection which project strongly on to the Madden-Julian Oscillation. The event in May witnessed the collapse of the trade winds across almost the entire Pacific Ocean, and was associated

Fig. 3 Time-longitude (Hovmoller) section of outgoing long-wave radiation averaged from 7.5°S to 7.5°N starting August 2001. The shading is the actual observed daily outgoing long-wave radiation anomalies, smoothed in time by a 7-day running mean, and smoothed in space by a R21 spherical spectral truncation. These are anomalies with respect to the long-term mean and annual cycle. Contoured are the anomalies associated with the Madden-Julian Oscillation following Wheeler and Kiladis (1999).



with anomalous warming of 1 to 2°C in sea-surface temperatures (SSTs). In facilitating the transition to El Niño conditions, this anomalous warming led to the 28.5°C SST isotherm shifting some 20° east in a period of weeks, such that it lay near 145°W in mid-June. Interestingly, such a shift is near the average of that observed at the peak of the post 1950 El Niño events described in Larkin and Harrison (2002), confirming the rapid establishment of El Niño conditions during the season.

The Hovmoller diagram suggests that the convective signal associated with the subsequent Madden-Julian Oscillation event in June/July was modified by the anomalous SSTs which enabled a greater eastward penetration of convection and anomalous westerlies (not shown). The remainder of winter witnessed only weak intraseasonal activity, with a persistent enhancement of convection near the date-line and suppression to the east as is typical of El Niño events (e.g., Hoerling et al. 1997).

Oceanic patterns

Sea-surface temperatures

Figure 4 shows winter 2002 SST anomalies in degrees Celsius (°C), as computed by the National Meteorological and Oceanographic Centre (NMOC). The contour interval is 0.5°C. Positive anomalies are shown in orange and red shades, while negative anomalies are shown in blue shades.

Reflecting the El Niño conditions which became established during the season, SSTs were warmer than average across most of the tropical Pacific, with a large area exceeding +1°C and locally approaching +2°C. The seasonal mean anomalies of the Niño 3 and 4 regions were +0.6°C and +0.95°C respectively. These values represent an anomalous warming of 0.5 to 1.5°C from autumn (Fawcett and Trewin 2003). Further east, SSTs along the South American coast were slightly cooler than normal, possibly in response to local southeasterly wind anomalies in this region. The pattern of the positive SST anomalies peaking in central parts of the Pacific with near normal SSTs near the South American coast was to persist through the 2002/03 El Niño event (Watkins 2003). As a consequence, projections of the SSTs onto the canonical pattern of SST anomalies characteristic of past El Niño events (e.g., Tourre and White 1995; Drosowsky and Chambers 2001) were suggestive of a relatively weak El Niño event overall, even though anomalies in the Niño 4 index region (which are strongly correlated with Australian rainfall) were very similar to those observed at the peak of the strong 1997/98 El Niño event.

Away from the Pacific, SSTs continued to be warmer than normal across almost the entire Indian Ocean during winter, as indeed they have been for most of the past few years. In the extra-tropics the pattern of anomalies was complex, at least in part reflecting the complexity of high latitude pressure anomalies during the season (see below).

Subsurface patterns

Figure 5 shows a time-longitude Hovmoller diagram of the anomaly in metres of the depth of the 20°C isotherm along the equatorial Pacific Ocean between January 1996 and August 2002, as calculated by the Bureau of Meteorology Research Centre (BMRC). This isotherm is generally situated very close to the equatorial ocean thermocline, the region of greatest temperature gradient with respect to depth. The thermocline can also be regarded as the boundary between the upper ocean warm water and the deeper ocean cold water. An abnormally shallow thermocline in the eastern Pacific Ocean is characteristic of La Niña events. Positive anomalies correspond to the

Fig. 4 Anomalies of sea-surface temperature for winter (June, July, August) 2002. The contour interval is 0.5°C.

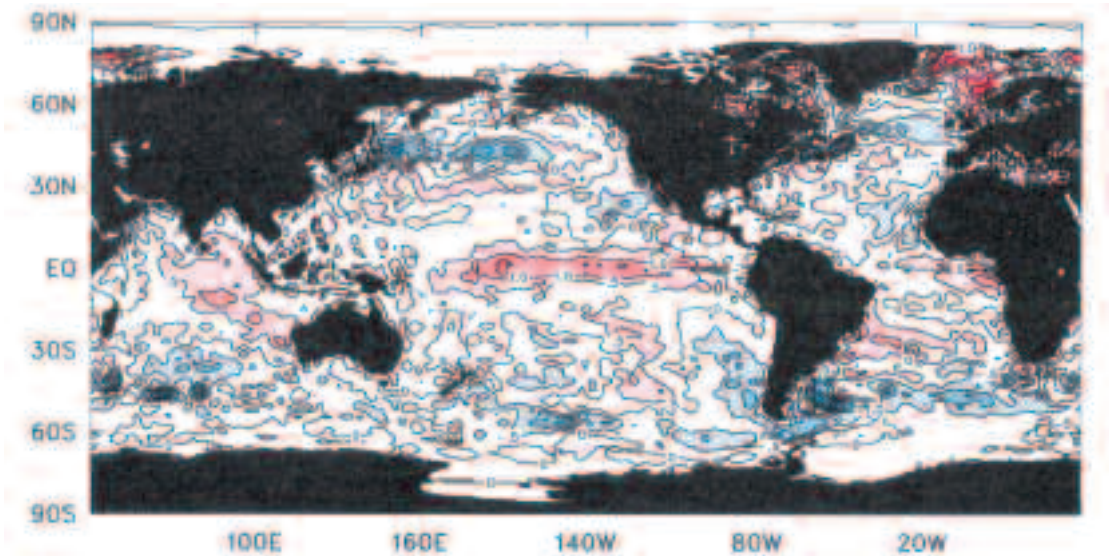
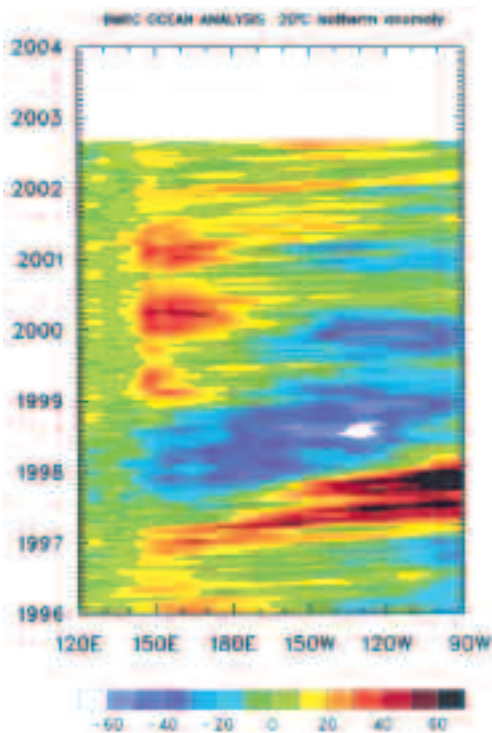


Fig. 5 Time-longitude section of the monthly anomalous depth of the 20°C isotherm at the equator from January 1996 to August 2002. The contour interval is 10 m.



20°C isotherm being deeper than average, and negative anomalies to it being shallower than average.

Three distinct Kelvin waves are evident in the Hovmoller, associated with westerly wind bursts in late 2001 (Gamble 2003), May and June/July 2002. Reflecting the consolidation of the El Niño event towards season's end, the associated transitional deepening of the thermocline was replaced with persistent anomalies which continued through to year's end (Watkins 2003), being the thermocline signature of the El Niño event.

Figure 6 shows a sequence of equatorial Pacific vertical temperature anomaly profiles for the four months ending August 2002, obtained from the NMOC. In the figure, red (blue) shades indicate subsurface waters which are warmer (cooler) than average. The ocean warming and deepening of the thermocline is clearly apparent in the transition from May to June, with relatively warm subsurface waters consolidating through July and August during which anomalies approached +3°C at depth. Such anomalies can be contrasted with those observed at the same time during the 1997/98 El Niño event which locally exceeded +7°C near the thermocline around 130°W. However, in the vicinity of the date-line, the anomalies are very similar in the two events being in the range of +1 to +2°C.

Atmospheric patterns

Surface analyses

The winter 2002 mean sea-level pressure (MSLP)

Fig. 6 Four-month February to August 2002 sequence of vertical temperature anomalies at the equator for the Pacific Ocean. The contour interval is 0.5°C.

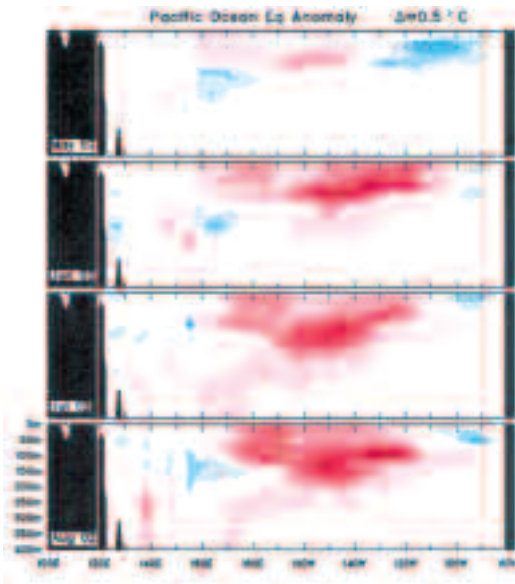


Fig. 7 Winter 2002 mean sea-level pressure (hPa). The contour interval is 5 hPa, with values above 1025 hPa and below 990 hPa stippled.

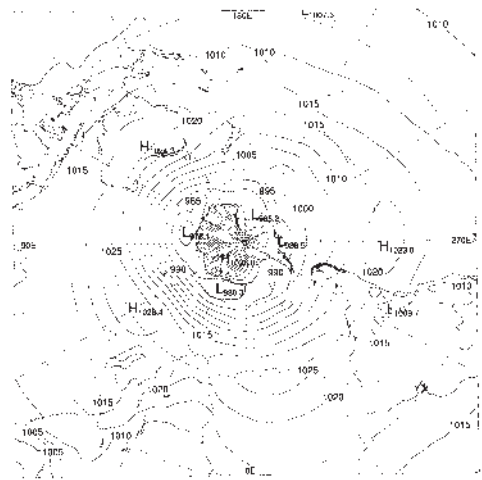
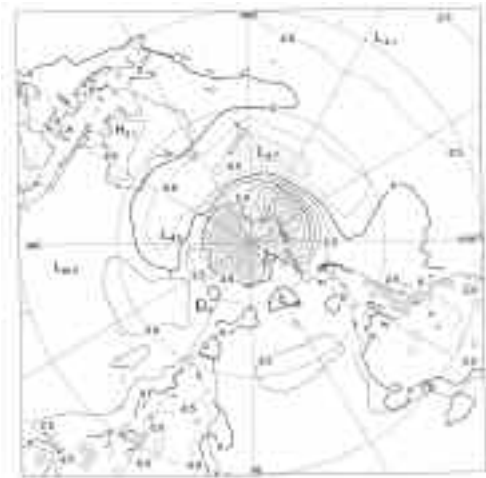


Fig. 8 Winter 2002 mean sea-level pressure anomaly (hPa). The contour interval is 2.5 hPa, with values above 5 hPa and below -5 hPa stippled.



across the southern hemisphere is shown in Fig. 7, with the associated anomalies shown in Fig. 8. These anomalies are the departures from an eleven-year (1979-1989) climatology obtained from the European Centre for Medium-range Weather Forecasts (ECMWF). The MSLP analysis itself has been computed using data obtained from the Commonwealth Bureau of Meteorology's Global Assimilation and Prediction (GASP) model daily 0000 UTC analyses. The MSLP anomaly field is not shown over areas of elevated topography.

The Antarctic circumpolar trough showed three substantial minima, located at 30°E, 100°E and 160°W, with weaker minima near the Weddell and Bellingshausen Seas. For the most part, the pattern of seasonal mean pressure at mid to high latitudes was close to the climatological average for winter, taking the form of a general three/four wave pattern.

The most noteworthy feature of the anomalous MSLP is the dipole between the central/eastern tropical Pacific and the Australian region, characteristic of El Niño events. In the Australian region, these anomalies implied a stronger than normal subtropical ridge and reduced frontal activity impacting continental Australia. Further south, pressures were lower than normal from around 90°E eastwards to nearly 90°W with an embedded strong cyclonic

anomaly east of New Zealand. Near Australia, the anomalously low pressures over the Southern Ocean combined with higher pressures over the continent to produce anomalous westerly flow in southern coastal parts (see Fig. 13).

Mid-tropospheric analyses

The mean 500 hPa geopotential height patterns for winter 2002 are shown in Fig. 9, with anomalies

Fig. 9 Winter 2002 500 hPa geopotential height (gpm). The contour interval is 100 gpm.

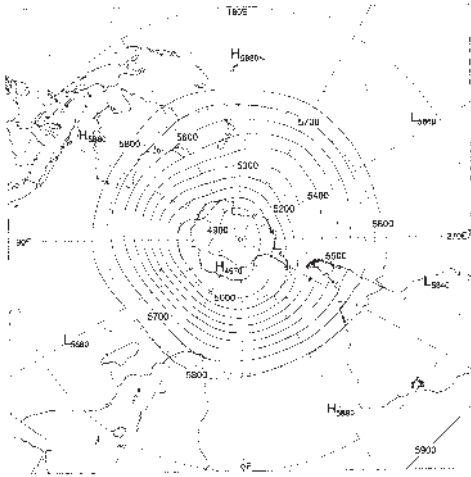
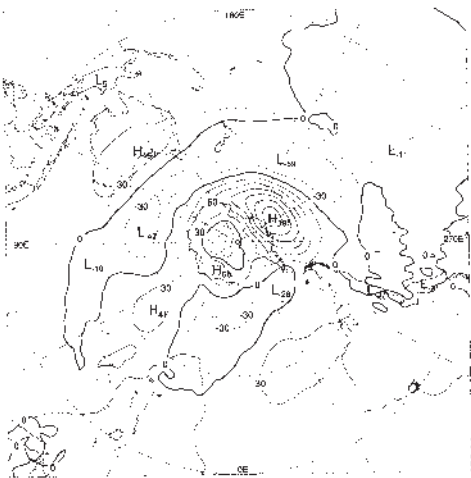


Fig. 10 Winter 2002 500 hPa geopotential height anomaly (gpm). The contour interval is 30 gpm, with values above 90 gpm and below -90 gpm stippled.



shown in Fig. 10. The characteristics in the MSLP pattern (Fig. 7) were also present at the mid-troposphere level (Fig. 9), with significant troughs (or lows) coinciding with the circumpolar minima in the pressure. In the anomaly field, the strengthened subtropical ridge across Australia was particularly strong at

the 500 hPa level, with the greatest anomalies shifted well south of those at the surface. In the central and eastern Pacific, heights were generally a little below normal and not as pronounced as the anomalies at the surface, consistent with historical El Niño events (e.g., Karoly 1989). Indeed, in the upper troposphere (e.g., 200 hPa) heights across most of the Pacific were anomalously high reflecting increased tropospheric thicknesses/temperatures.

Blocking

Figure 11 is a time-longitude section of the daily southern hemisphere mid-level Blocking Index,

$$BI = 1/2[(u_{25} + u_{30}) - (u_{40} + 2u_{45} + u_{50}) + (u_{55} + u_{60})].$$

Here, u_{λ} indicates the 500 hPa level zonal wind component at 1 degrees of southern hemisphere latitude ranging from 0° at the equator to +90°S at the South Pole. The blocking index measures the strength of the 500 hPa flow at the mid-latitudes (40°S to 50°S) relative to that at subtropical (25°S to 30°S) and high (55°S to 60°S) latitudes.

Taken across the season in the form of a seasonal mean (Fig. 12), blocking was significantly below normal from near 90°E to 120°W, largely reflecting the enhanced mid latitude height gradient shown previously (Fig. 10). Elsewhere, blocking activity was near the seasonal mean except in the vicinity of the Atlantic Ocean where it was slightly lower than normal. Consistent with the mean, individual blocking events were relatively infrequent and short lived across the southern hemisphere.

Winds

Low-level (850 hPa) and upper-level (200 hPa) wind anomalies for winter 2002 are shown in Figs 13 and 14 respectively. Consistent with the anomalous MSLP, the western and central Pacific experienced westerly wind anomalies amounting to some 2 to 5 m s⁻¹ with a well developed region of anomalous convergence near the date-line. This region of convergence was associated with enhanced tropical convection as described previously. Further east, the trades were near to slightly stronger than normal.

Low-level wind anomalies in the Australian region followed the MSLP anomaly pattern, with enhanced westerlies to Australia's south, extending well into the Pacific Ocean. An enhancement of the low-level westerlies through this region is a feature common to many El Niño events (Jones and Simmonds 1994; Jones and Trewin 2000), and gives rise to relatively weak correlations between rainfall and the SOI in places such as western Tasmania.

Fig. 11 Winter 2002 daily blocking index: time-longitude (Hovmoller) section. The horizontal axis measures degrees of longitude east of the Greenwich meridian. Day one is 1st June 2002.

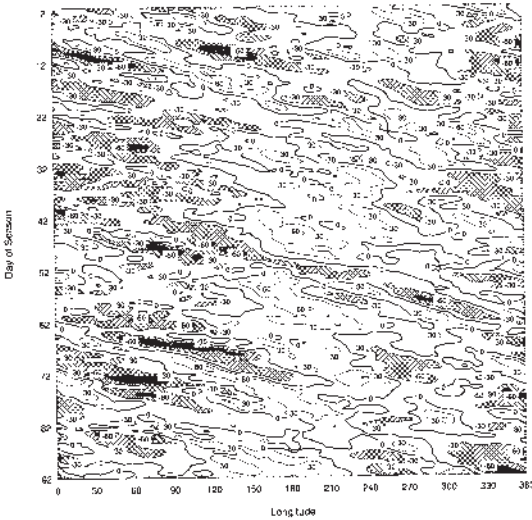
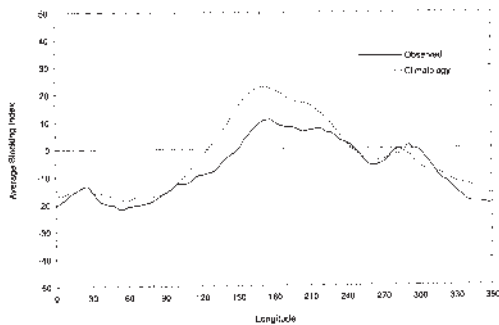


Fig. 12 Mean southern hemisphere blocking index for winter 2002 (solid line). The dashed line shows the corresponding long-term average. The horizontal axis shows degrees east of the Greenwich meridian.



At the upper levels the anomaly patterns show a marked wave train with an upper anticyclone to the near south of the Niño 4 region, a cyclonic anomaly southeast of New Zealand and a second anticyclonic anomaly near the Amundsen Sea. The tropical/sub-tropical anticyclonic anomaly lies to the near south of the core of anomalous convection and tropospheric

Fig. 13 Winter 2002 850 hPa vector wind anomalies with contours of vector magnitude overlaid. The contour interval is 5 m s^{-1} , with values above 5 m s^{-1} stippled.

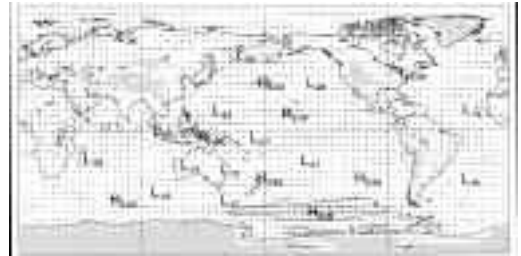
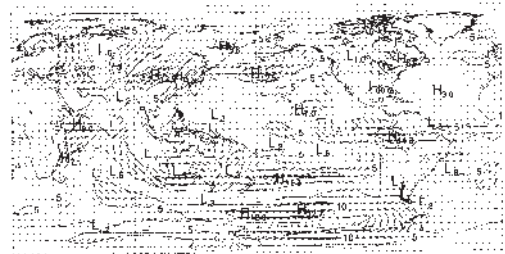


Fig. 14 Winter 2002 200 hPa vector wind anomalies with contours of vector magnitude overlaid. The contour interval is 5 m s^{-1} , with values above 5 m s^{-1} stippled.



heating during winter 2002, associated with the warmer than normal SSTs in the tropical central Pacific. This overall pattern of anomalies shows a remarkable similarity to the canonical El Niño structure described by Karoly (1989), underscoring the capacity for tropical anomalies to strongly influence the extratropics.

Over Australia, a well-developed anomalous anticyclone was associated with enhanced westerlies in the mid latitudes and anomalous easterlies in the subtropics. The anomalous subtropical easterlies are consistent with the lack of northwest cloud band activity through the winter season which contributed to the observed severe drought conditions.

Australian region

Rainfall

Figure 15 shows the winter rainfall totals for Australia, while Fig. 16 shows the autumn rainfall

Fig. 15 Winter 2002 rainfall totals for Australia (mm).

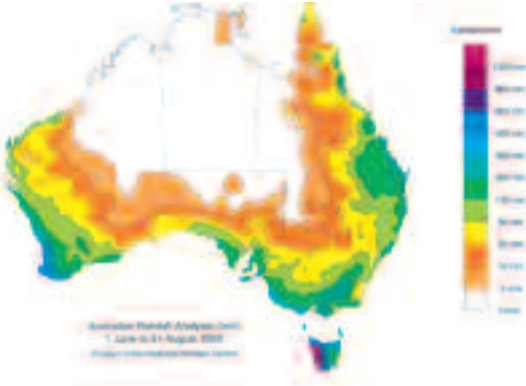
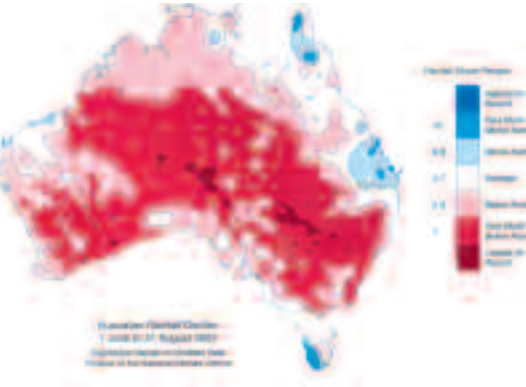


Fig. 16 Winter 2002 rainfall deciles for Australia: decile range values based on grid-point values over the winters 1900 to 2002.



deciles, where the deciles are calculated with respect to gridded rainfall data for all winters from 1900 to 2002.

Winter rainfall was below average (deciles 1 to 3) across most of the continent, with extensive areas of very much below average (decile 1), and small areas of lowest on record. Areally, 91 per cent of Australia recorded rainfall below the median for the season, while 46 per cent recorded rainfall in the lowest decile. Across Australia the mean winter rainfall of 36mm was the sixth lowest since 1900, and only 9mm above the record low set in 1982. Underscoring the influence of the El Niño in large scale wintertime droughts over Australia, of the five winters drier than 2002 (being 1982, 1940, 1976, 1977 and 1994) each were during El Niño events (Reid 2003).

Against this background of very dry conditions, parts of coastal Queensland, central Western Australia, and western Tasmania experienced above average seasonal rains. The region of above average rainfall on the central Queensland coast was the result of good rains in early June and again in mid/late August. Indeed, the rain during August which locally amounted to more than 250mm in a week resulted in a number of stations recording their wettest August on record. It is notable that during the intervening month of July, this same region experienced very dry conditions, with totals for the month being locally the lowest on record.

Further south, very wet conditions were recorded through western Tasmania for the season (wettest on record in the far southwest), with well above normal rainfall in each of the three winter months, in association with the persistently enhanced westerlies which the area experienced. Finally, the area around Exmouth in Western Australia experienced extraordinarily heavy rain between the 3rd and 5th of June, with 304.6mm falling on June 4th alone. The rainfall on this day was 194mm above the previous June daily record, and indeed greater than the long-term mean annual total of 277mm.

Taken as a whole, the very poor winter rains over most of Australia intensified and expanded the drought which became established in March/April 2002. This drought would eventually prove to be one of Australia's severest El Niño drought episodes on record.

Temperatures

Figures 17 and 18 show the maximum and minimum temperature anomalies for winter 2002, respectively. The anomalies have been calculated with respect to the 1961-1990 period.

Maximum temperatures were above average for the season across almost all of the country (Fig. 17), with the exception of parts of the tropics and small areas of southwest Western Australia and southeast Queensland. Across much of Australia, maximum temperatures were more than 1°C above the average for the 1961-90 period. Peak anomaly values occurred in Western Australia and inland parts of eastern Australia with values locally exceeding +2.5°C. These can be compared to the standard deviation of winter mean maximum temperature which is in the range of 0.6 to 1.0°C (Jones 1999), implying positive anomalies widely in the range of 2 to 5 standard deviations. Not surprisingly, much of central and eastern Australia experienced its warmest maximum temperatures in records dating back to 1950. Some of the area which experienced its warmest winter on record also experienced its warmest July on record.

Fig. 17 Winter 2002 maximum temperature anomalies for Australia based on a 1961-1990 mean (°C).

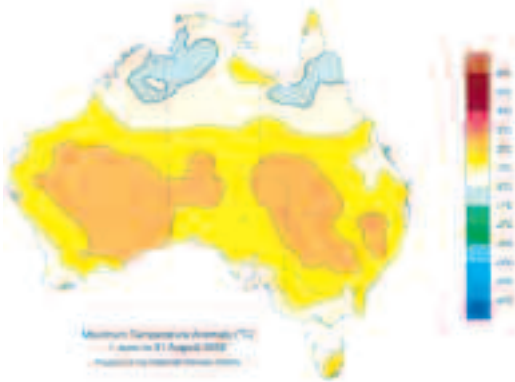


Fig. 18 Winter 2002 minimum temperature anomalies for Australia based on a 1961-1990 mean (°C).



In area-averaged terms for Australia, 2002 was the warmest winter of the post-1950 period by a substantial margin, with a seasonal anomaly of $+1.41^{\circ}\text{C}$, compared with the previous record of $+0.96^{\circ}\text{C}$, set in 1996. In some contrast to the extreme monthly values experienced during autumn however, only the month of July came close to setting a monthly temperature record (in area-averaged terms; $+1.94^{\circ}\text{C}$ against a record of $+1.97^{\circ}\text{C}$ in 1975). Rather, each month displayed persistent warmth, with a national anomaly value greater than $+1^{\circ}\text{C}$ – this being the first winter on record that this has occurred. Regionally it was the warmest winter of the post-1950 period for New

South Wales, Victoria, South Australia and Western Australia (again, in area-averaged terms). Anomalously high winter daytime temperatures are a well known characteristic of past El Niño events, being a result of increased shortwave radiation and decreased surface latent cooling (see for example, Jones and Trewin 2000). However, the anomalies observed during winter 2002 were approximately 0.5 to 0.8°C higher than one would expect from past relationships between Australian rainfall and maximum temperatures. A partial explanation for the apparent discrepancy lies in the warming trend which has been observed in Australian maximum temperatures since 1910 and particularly since 1950. This warming has amounted to $0.6 \pm 0.3^{\circ}\text{C}$.

As a direct result of the low cloudiness and rainfall, the diurnal temperature range anomaly across Australia was a record $+2.1^{\circ}\text{C}$ during winter 2002, exceeding the previous record of $+1.5^{\circ}\text{C}$ set in 1976. As a consequence, minimum temperatures were widely below normal during the season, with particularly cool temperatures observed in parts of the subtropics and tropics where negative anomalies locally exceeded 4°C in magnitude, with below normal night temperatures prevalent in each of the three winter months. About parts of the Top End and Gulf of Carpentaria, the seasonal mean minimum temperatures were the lowest in records dating back to 1950. In the south, departures of the minimum temperature were modest, with most areas within 1°C of the 1961-1990 average. The all-Australian minimum temperature anomaly was -0.7°C , which ranks tenth in 53 years of records. While being negative, it is noteworthy that the similarly dry years of 1976, 1977, 1982 and 1994 were all cooler than 2002.

Combining maximum and minimum temperatures, the seasonal mean temperature anomaly for winter for Australia was a relatively unremarkable $+0.4^{\circ}\text{C}$.

References

- Commonwealth Bureau of Meteorology 2002. *Climate Monitoring Bulletin - Australia*, June, July and August 2002 issues. National Climate Centre, Bur. Met., Australia.
- Climate Prediction Center 2002. *Climate Diagnostics Bulletin*, June, July and August 2002 issues. US Department of Commerce, National Oceanic and Atmospheric Administration, Washington D.C.
- Drosowsky, W. and Chambers, L.E. 2001. Near global sea surface temperature anomalies as predictors of Australian seasonal rainfall. *Jnl climate*, 14, 1677-87.
- Fawcett, R.J.B. and Trewin, B.C. 2003. Seasonal climate summary southern hemisphere (autumn 2002): onset of El Niño conditions. *Aust. Met. Mag.*, 52, 127-36.
- Gamble, F.M. 2003. Seasonal climate summary southern hemisphere (summer 2001/02): a continuation of near-normal conditions in the tropical Pacific. *Aust. Met. Mag.*, 52, 63-72.

- Hoerling M.P., Kumar, A. and Zhong, M. 1997. El Niño, La Niña, and the nonlinearity of their teleconnections. *Jnl climate*, 10, 1769-86.
- Jones, D.A. 1999. Characteristics of Australian land surface temperature variability. *Theor. Appl. Climatol.*, 63, 11-31.
- Jones, D.A. 2002. The 2002 El Niño and its impacts on Australia. *Bull. Aust. Met. Soc.*, 15, 91-5.
- Jones, D.A. and Simmonds, I. 1994. A climatology of Southern Hemisphere anticyclones. *Climate Dynamics*, 10, 333-48.
- Jones, D.A. and Trewin, B.C. 2000. On the relationships between the El Niño-Southern Oscillation and Australian land surface temperature. *Int. J. Climatol.*, 20, 697-719.
- Karoly, D.J. 1989. Southern Hemisphere circulation features associated with El Niño-Southern Oscillation events. *Jnl climate*, 2, 1239-52.
- Larkin, N.K. and Harrison, D.E. 2002. ENSO warm (El Niño) and cold (La Niña) event life cycles: ocean surface anomaly patterns, their symmetries, asymmetries, and implications. *Jnl climate*, 15, 1118-40.
- Reid, P.A. 2003. An operational definition of El Niño. *Proceedings 7th Int. Conf. on Southern Hemisphere Meteorology and Oceanography*, Wellington N.Z., 128-129.
- Tourre, Y.M. and White, W.B. 1995. ENSO signals in global upper-ocean temperature. *J. Phy. Oceanogr.*, 25, 1317-32.
- Watkins, A.B. 2003. Seasonal climate summary southern hemisphere (spring 2002): *Aust. Met. Mag.*, 52, 213-226.
- Wheeler, M. and Kiladis, G.N. 1999. Convectively coupled equatorial waves: analysis of clouds and temperature in the wavenumber-frequency domain. *J. Atmos. Sci.*, 56, 374-399.

Appendix

Data sources used for this review were:

- National Climate Centre, *Climate Monitoring Bulletin* - Australia. Obtainable from the National Climate Centre, Commonwealth Bureau of Meteorology, GPO Box 1289K, Melbourne, Vic. 3001, Australia.
- Climate Prediction Center (CPC), *Climate Diagnostics Bulletin*. Obtainable from the Climate Prediction Center (CPC), National Weather Service, Washington D.C., 20233, USA.